



Assessment of fouling in commonly used polymeric membranes

Iosif Marios Scoullou, Ioannis Tournis, Evangelos Kouvelos, Zili Sideratou, Andreas Sapalidis*

Institute of Nanoscience and Nanotechnology, National Centre for Scientific Research “Demokritos”, Patr. Gregoriou & 27 Neapoleos Str., 153 41 Agia Paraskevi Attikis, Greece, Tel. +30-2106503977; emails: a.sapalidis@inn.demokritos.gr (A. Sapalidis), i.scoullou@inn.demokritos.gr (I.M. Scoullou), i.tournis@inn.demokritos.gr (I. Tournis), v.kouvelos@inn.demokritos.gr (E. Kouvelos), z.sideratou@inn.demokritos.gr (Z. Sideratou)

Received 25 August 2021; Accepted 28 December 2021

ABSTRACT

The formation of biofouling on membrane surfaces is a critical factor that affects the efficiency of desalination processes, because it creates operational problems and increases the energy and cleaning requirements. This research studies the efficacy of different membranes in inhibiting the adhesion of proteins and bacteria on their surface. The adhesion of bovine serum albumin (BSA) and of *Escherichia coli* DH5 α was studied on four membrane types: polytetrafluoroethylene, polyvinylidene fluoride, polyethersulfone and polyamide. Evaluation was performed by using 1 g L⁻¹ BSA and a suspension of 10⁵ CFU mL⁻¹ of *E. coli* on both static and dynamic setup. Subsequently, the membranes were mildly washed with distilled water to remove weakly attached cells and the concentration of the fouling agent was determined. The results indicate that the adhesion of both agents is stronger on the hydrophilic membrane surfaces compared to the hydrophobic ones.

Keywords: Biofouling; Membranes; Hydrophobicity; Bovine serum albumin; *Escherichia coli*

1. Introduction

Global clean water scarcity and the rising demand of water usable for domestic and industrial use requires efficient and low-cost water purification technologies. Membrane-based separation processes, such as reverse osmosis, tend to be established as the main technologies not only for seawater desalination, but also for the treatment of various waste streams [1,2]. Membrane-based processes are easy to handle, have well-arranged process conditions and their efficiency depends entirely on the membrane itself [3]. Nevertheless, membrane desalination is energy intensive, with high pressure pumps being responsible for more than 40% of the total expenditures and up to 80% of the overall power consumption of the membrane desalination plants [4]. Membrane fouling has been

identified as the major drawback in the effort to increase membrane desalination process efficiency at commercial scale in terms of sustainability and cost [5]. Membrane fouling can be categorized into organic fouling, particle/colloidal fouling, scaling/inorganic fouling and biofouling [6]. Biofouling is the growth of microorganisms in the membrane system by utilizing the biodegradable substances from the water phase and converting them into metabolic products and biomass, frequently forming a biofilm [7]. It accounts for more than 45% of all fouling cases and causes the degradation of plant operations by reducing flux rates, increasing the volume of reject water, increasing energy consumption and ultimately causing the premature replacement of membrane elements [8]. In some instances, microorganisms of the biofilm might infiltrate

* Corresponding author.

the membranes and enter into the permeate stream, leading to the deterioration of the produced water quality [9]. Also, the excretion of acid from biofilms can result in biodegradation of the membranes, particularly of cellulose acetate [10]. Pre-treatment procedures such as pre-filtration [11] and dosing of biocides [12] are applied, however, their effectiveness against biofouling is limited due to the rapid self-reproducing nature of microorganisms [13] and the use of chemical methods has adverse effects on the environment and on human health. Therefore, together with process optimisation, membrane surface modification is the key to minimise biofouling [14,15]. In order to assess the degree in which different membrane surfaces are prone to organic and biological fouling, apart from predicting the fouling potential of feed waters [16] and using microscopic and spectroscopic techniques that allow visualisation of the biofilms and their structure after they are established [17], most other methods used are specific for each fouling agent studied.

The objective of this work is to better understand the effect of different membrane materials on the protein and bacterial adhesion on their surface in order to facilitate ultimately the selection of antifouling membranes for reducing costs and energy consumption of the desalination process. The adhesion of a model protein, bovine serum albumin (BSA), and of biofilm-forming gram-negative bacteria *E. coli*, both of which have been widely used in membrane fouling research [18,19], were studied on four membrane types. Furthermore, four different methods were used for the evaluation of organic and biological fouling. Fouling was studied both static, in the absence of flux and pressure, and dynamic, approaching the real operating conditions of the membranes.

2. Materials and methods

2.1. Membranes characterisation

Four membrane types were tested, two hydrophobic ones, polytetrafluoroethylene (PTFE) and polyvinylidene fluoride (PVDF), and two hydrophilic ones, polyethersulfone (PES) and nylon. The PTFE membranes (Filtres Fioroni, Ingré, France), the PVDF membranes (Durapore, Merck, Darmstadt, Germany) and the polyamide (PA/nylon) membranes (Filtres Fioroni, Ingré, France) used had a nominal pore size of 0.22 μm . The PES membranes (Sterlitech, Kent, WA, USA) used had a nominal pore size of 1.2 μm . All the membranes had a diameter of 47 mm.

The measurement of water and of BSA solution contact angle of the membranes took place using the sessile drop technique with Drop Shape Analyzer (KRÜSS, Hamburg, Germany). The drop volume of distilled (DI) water and of the BSA solution was 4 μL . An average of the left and right contact angles was considered as the mean contact angle and the measurements were carried out at least four times on each membrane type, at room temperature.

2.2. Indicator organism

The organism of study was *Escherichia coli* (DH5 α). Before each batch experiment *E. coli* was incubated in LB

(Luria–Bertani) broth [10 g L⁻¹ tryptone (peptone from casein, Fermtech, Merck KGaA, Darmstadt, Germany), 5 g L⁻¹ yeast extract (MP Biomedicals, LLC, Solon, OH, USA), 10 g L⁻¹ NaCl (Penta s.r.o., Prague, Czech Republic), with addition of 200 μL NaOH 5 N to achieve a pH of 7.5 for 24 h at 37°C. After incubation, the concentration of the inoculum was around 3.3×10^9 CFU mL⁻¹. A first dilution step was performed in LB broth to achieve 10^8 CFU mL⁻¹ and subsequently in DI water to achieve the required initial concentration for the experiments, that of 10^5 CFU mL⁻¹.

The enumeration was performed by spreading 0.1 mL of the suspension in duplicates on LB agar [15 g L⁻¹ agar, USP grade (MP Biomedicals, LLC, Solon, OH, USA) in LB medium] plates followed by 24 h of incubation at 37°C. The necessary dilution steps took place with the use of LB broth. All the media used were sterilised by autoclaving at 121°C for 15 min.

2.3. Experimental design

2.3.1. Protein adsorption

Bovine serum albumin (BSA) (Acros Organics, Fair Lawn, New Jersey, United States) was used as model protein to evaluate protein adsorption on the investigated membranes in phosphate buffered saline (PBS) (0.1 mol L⁻¹, pH 7.4). The membrane samples (one for each membrane type) were cleaned with PBS under ultrasonication for 30 min and subsequently they were immersed in PBS solution containing BSA (1 g L⁻¹) at 25°C for 24 h. The protein concentration before and after the adsorption was measured by a Cary 100 Conc. UV-Vis spectrophotometer (Varian, Inc., Palo Alto, California, USA) at 280 nm and the amount of adsorbed BSA was calculated by comparing the absorption intensity variation.

2.3.2. Protein fouling

Protein fouling was tested in the setup presented in Fig. 1. The flux of BSA (1 g L⁻¹) solution (PBS 0.1 mol L⁻¹, pH 7.4) through each membrane was measured and the fouling ratio (R_f), defined as the degree of flux loss caused by fouling, was calculated as follows:

$$R_f = \left(1 - \frac{J_{30}}{J_0}\right) \times 100\% \quad (1)$$

where J_0 is the initial flux of the BSA solution at the beginning of the batch test ($\text{L m}^{-2} \text{h}^{-1}$) and J_{30} is the flux of the BSA solution after a single pass for 30 min ($\text{L m}^{-2} \text{h}^{-1}$) run time.

Total fouling is the sum of reversible fouling caused by concentration polarisation plus irreversible fouling caused by adsorption or deposition of protein molecules on the membrane surface [20].

2.3.3. Bacterial attachment (static)

The membranes were dipped (in duplicate) for 5 min in 40 mL of an *E. coli* suspension of 10^5 CFU mL⁻¹. Taking into account the area of the membranes, the initial inoculum was 3.4×10^4 CFU on top of each membrane. After each test, the

membranes were mildly washed by being dipped thrice in 200 mL of DI water to remove weakly attached cells.

Sampling was performed by swabbing. Sterile cotton tipped swabs with plastic stick (Jiangsu Rongye Technology Co., Ltd., Touqiao, Jiangsu, China) were used to collect samples from all membranes (duplicate membranes for each material). Each swab was applied 20 times in one direction (from left to right and then from right to left) and 20 times in a 90° perpendicular direction with regard to the first swabbing direction (from the front to the back and vice versa). The swabs were held so that the handle created an about 30° angle with respect to the surface, they were rotated slowly each time and, as much as possible, a similar pressure was continuously applied. The swabs were submerged in a sterile tube with 2 mL of 0.1% peptone physiological salt solution to be moistened prior to swabbing. After sampling the swabs were stirred rigorously in the same solution as eluent and the suspension was plated for colony counting.

2.3.4. Bacterial attachment (dynamic)

The experimental design consisted of batch tests with all the membranes tried in duplicates. A volume of 100 mL of the *E. coli* suspension of 10^5 CFU mL⁻¹ was filtered with a constant feed pressure. The permeate stream was discarded and the concentrate was recycled back to the feed tank. The process flow diagram is similar to Fig. 1, with the difference that the concentrate was recycled.

Following each test, the membranes were mildly washed by being dipped thrice in 200 mL of DI water to remove weakly attached cells and subsequently placed in vials containing 10 mL on LB broth and were incubated for 16 h at 37°C under continuous stirring at 220 rpm. After incubation, the suspension was spread for enumeration by colony counting. In parallel, LB broth was incubated in the same conditions and plated as a control, to make sure that the medium was sterile. Furthermore, the inoculum suspension was also plated after the end of each batch experiment to account for any die-off of the bacteria.

2.4. Data analysis

To investigate whether the membranes used had a statistically significant effect on the concentrations of bacteria

counted, two-factor analysis of variance with replication (all the membranes were tested in duplicate) was performed for the log₁₀ values of the bacterial concentrations measured, with a significance level, α , of 0.05. The null hypothesis was that the concentrations of *E. coli* came from distributions with equal population means.

3. Results and discussion

3.1. Membrane characterisation

The contact angle of water was measured on all membranes in order to determine the hydrophobicity of the membranes. The two hydrophobic membranes, PTFE and PVDF, had mean contact angles of $128.45^\circ \pm 3.71^\circ$ and $122.56^\circ \pm 0.34^\circ$, respectively. The two hydrophilic membranes, PES and PA had contact angles of $38.18^\circ \pm 5.62^\circ$ and $34.56^\circ \pm 3.89^\circ$, respectively. The contact angles of the BSA solution were similar with water on the hydrophilic membranes and slightly higher than for water on the hydrophobic membranes. The pictures and the values can be seen in Table 1. It must be noted that since contact angle is affected by porosity [21], the contact angle of PES with pore size 1.2 μm is not directly comparable with that of nylon and of the other membranes which have a pore size of 0.22 μm .

In literature, the water contact angle of PTFE membranes (of mean pore size of 0.17 μm) was measured to be around 120° [22] and $128^\circ \pm 2^\circ$ [23], of PVDF membranes, $145^\circ \pm 2^\circ$ (nominal pore size 0.2 μm) [24], of PES membranes about 60° (pore size 2–5 nm) [25] and 52.3° (pore size 98 nm) [26], of a nylon 66 film 52.8° – 58.0° [27].

3.2. Protein attachment and fouling

The BSA amount adsorbed on the membranes, is calculated from the difference in BSA concentration in the solution before and after the period of exposure of the membranes and was calculated as 14.0, 15.0, 17.6 and 34.1 mg BSA per g of membrane respectively for PTFE, PVDF, PES and nylon, as is presented in Fig. 2.

Protein adhesion on membranes is one of the most important evidence in evaluating the fouling resistance of membranes [20]. The hydrophobic membranes showed better antifouling properties against BSA than the hydrophilic ones, as presented in Fig. 3 and Table 2.

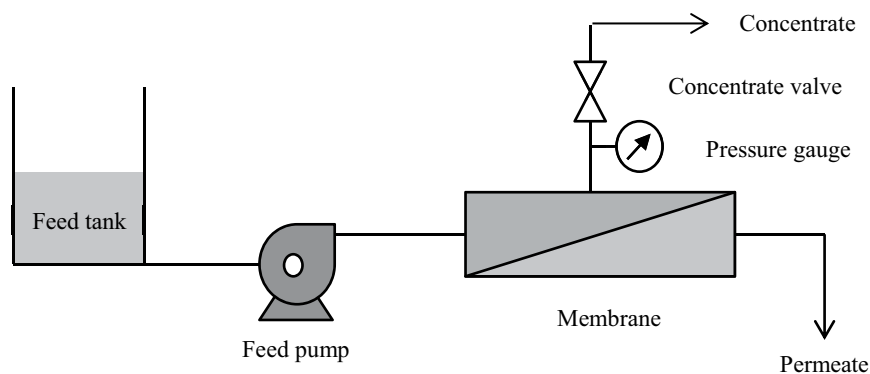
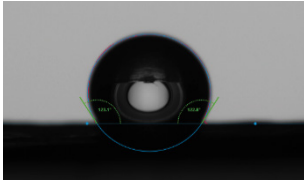
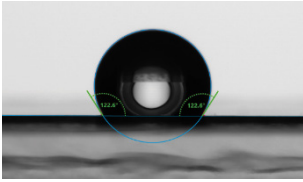
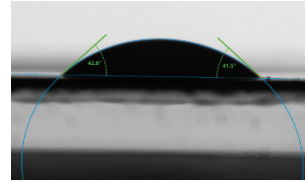
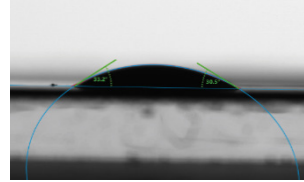
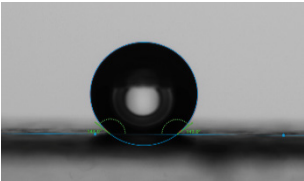
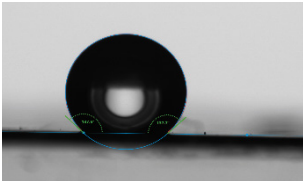
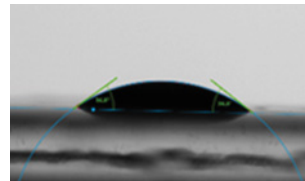
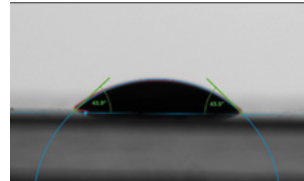


Fig. 1. Process flow diagram of the experimental setup.

Table 1
The measurement of water contact angles and BSA solution contact angles on PTFE, PVDF, PES and nylon membranes

	PTFE	PVDF	PES	Nylon
Water				
	128.45° ± 3.71°	122.56° ± 0.34°	38.18° ± 5.62°	34.56° ± 3.89°
BSA solution				
	143.40° ± 0.57°	137.60° ± 2.13°	36.80° ± 3.67°	41.00° ± 4.10°

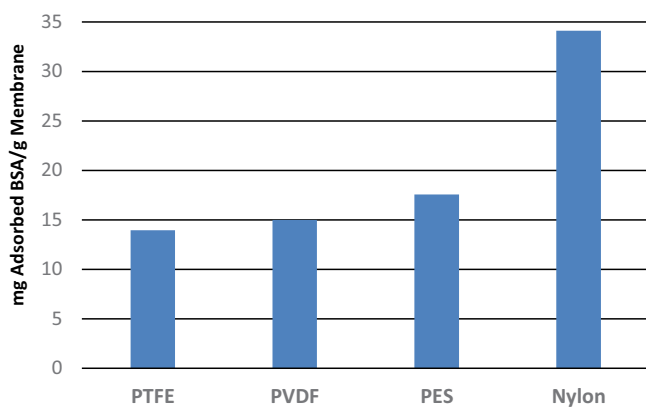


Fig. 2. The amount of BSA adsorbed on each membrane per weight of the membrane.

It can be seen from Fig. 3 that the flux on all membranes decreased by at least 70% in the first 30 min. Protein molecules in the feed solution, deposited or adsorbed on the membrane surface, cause a drop in flux rapidly during the first few minutes of operation, as was also observed by Stafie et al. [28]. The flux was reduced faster on the hydrophilic membranes compared to the hydrophobic ones with nylon in particular reaching a flux loss of more than 80% after 22 min. These observations agree to the conclusions of Jeyachandran et al. [29] that the adsorption and interaction of BSA molecules were much stronger on hydrophilic surfaces compared to hydrophobic ones. Findings from molecular modelling revealed that BSA molecules interact with hydrophobic surfaces through CH₃ group and with hydrophilic surface with polar –COOH groups [29].

Additionally, Zhang et al. [30] showed that the amount of fouling by humic acid was lower on PES membranes

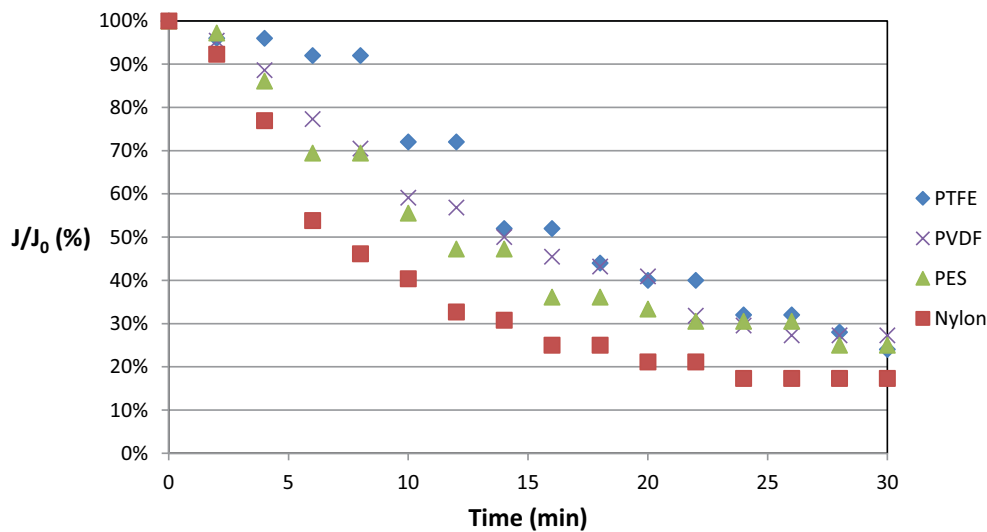


Fig. 3. Time courses of the flux (J) of the tested membranes during filtration of BSA solution normalised as divided by the flux at the beginning of each batch test (J_0).

Table 2
Experimental parameters of the tests for BSA adsorption

Membrane type	Initial permeance (LMH/bar)	Permeance@ 30 min (LMH/bar)	Permeance loss (%)	Initial recovery (%)	Recovery@ 30 min (%)	R_f %
PTFE	476	114	76.1	35.71	8.57	76.05
PVDF	943	257	72.8	62.86	17.14	72.74
PES	7,714	1,714	77.8	51.43	11.43	77.78
Nylon	2,228	386	82.7	74.29	12.86	82.68

Table 3
Experimental parameters of the batch tests for *E. coli* adsorption (dynamic experiment)

Membrane type	Permeance ($L h^{-1} m^{-2} bar^{-1}$)	<i>E. coli</i> concentration (CFU mL^{-1})
PTFE	720	5.7×10^8
PVDF	2,220	4.5×10^8
PES	75,480	9.4×10^8
Nylon	5,280	14.4×10^8

modified by hydrophobic additives compared to unmodified ones. Choo and Lee [31] reported that the most hydrophobic PVDF showed smaller fouling tendency than polysulfone and cellulose acetate (CA) membranes, during filtration of anaerobic digestion broth, while Chen et al. [32] concluded that the flux decrease rate of the membranes followed the order CA > PVDF > PES membranes, with CA being the most hydrophilic one among them.

On the other hand, it has been claimed that hydrophobic surfaces are in general more prone to initial bacterial adhesion and biofouling compared to hydrophilic ones [21] and that fouling increases with an increase in the hydrophobicity of polymer surfaces [33]. This assumption is reasonable in the case of hydrophobic organic molecules which are attracted towards hydrophobic surfaces, but it is not safe to extrapolate any correlation to all fouling agents or to extremely hydrophilic or hydrophobic surfaces [33]. It is noteworthy that both super-hydrophobic and super-hydrophilic surfaces may present antifouling properties; the first by supporting a thin air layer between the membrane and the water phase, and the latter by preferring contact with water than with fouling agents [34]. This supports the fact that surface hydrophobicity itself is not enough to evaluate the extent of fouling [31], as the fouling behavior of membranes can only be predicted from the combined knowledge of solution chemistry, surface chemical properties and surface morphology [32].

3.3. Bacterial attachment: static and dynamic experiments

For the static tests, the membranes were dipped in the *E. coli* suspension and were subsequently mildly washed. Sampling was performed by swabbing and the results are presented in Fig. 4.

The population of *E. coli* on both hydrophobic membranes was found to be below the detection limit of 20 CFU, while on the hydrophilic membranes at least 1% of the

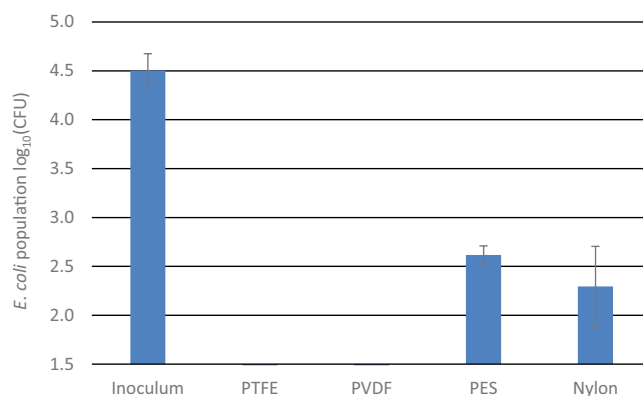


Fig. 4. The population of *E. coli* in the inoculum suspension and as detected on the surface of each membrane (static experiment).

inoculum concentration was detected on the membrane surfaces.

The results of the microbiological tests of the dynamic experiment can be seen in Fig. 5 and Table 3.

The statistical analysis of the results with analysis of variance showed that the differences in *E. coli* concentrations between different membrane types were statistically significant ($p = 0.005$). Also, as it was expected, the duplicate samples for each membrane type had no significant difference ($p = 0.18$).

First of all, it is assumed that *E. coli* cells did not infiltrate through any of the membranes because they have a size of approximately $1 \mu m \times 3 \mu m$ [35], larger than the pore size of the membranes used.

In general, it has been shown that hydrophilic bacteria prefer hydrophilic surfaces while hydrophobic bacteria prefer hydrophobic surfaces [21]. Van Loosdrecht et al. [36] measured the water contact angles of different bacteria collected on micropore filters, resulting in $15.7^\circ \pm 1.2^\circ$ for *E. coli* NCTC 9002 and $24.7^\circ \pm 0.4^\circ$ for *E. coli* K-12. Similar study conducted by Van der Mei et al. [37] on different cell lawns confirmed that all *E. coli* strains had hydrophilic water contact angles between 17° and 57° . Additionally, Zhang et al. [38] using surface free energy as a measure of cell surface hydrophobicity determined that *E. coli* DH5 α , the strain used in the current research, had a surface free energy of 65.1 mJ m^{-2} , classified as the most hydrophilic among the bacteria they studied. The above findings are in agreement with the results of this study where *E. coli* attachment was higher on the hydrophilic membranes compared to the hydrophobic ones in both the static and dynamic experiments.

Table 4
Summary of experimental parameters for the four membrane types tested

Membrane type	Pore size (μm)	Water contact angle ($^\circ$)	BSA adsorption (mg adsorbed BSA/g membrane)	Flux loss due to BSA fouling R_f (%)	<i>E. coli</i> population adsorbed on each membrane in the static experiment (CFU)	<i>E. coli</i> concentration in the dynamic experiment (CFU mL ⁻¹)
PTFE	0.22	128.45 \pm 3.71	14.0	76.0	<20	5.7 \times 10 ⁸
PVDF	0.22	122.56 \pm 0.34	15.0	72.7	<20	4.5 \times 10 ⁸
PES	1.2	38.18 \pm 5.62	17.6	75.0	4.2 \times 10 ²	9.4 \times 10 ⁸
Nylon	0.22	34.56 \pm 3.89	34.1	82.7	2.7 \times 10 ²	14.4 \times 10 ⁸

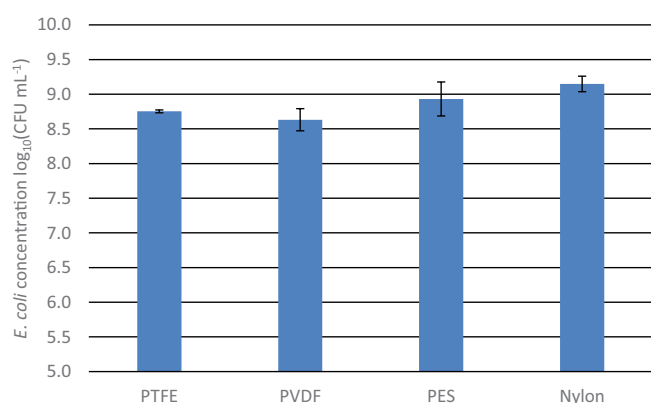


Fig. 5. The resulting *E. coli* concentrations after incubation of the membranes in LB broth for the four samples (dynamic experiment). Error bars indicate the standard deviation.

The overall results from all the experiments are summarised in Table 4.

3.4. Practical implications

This work aims to provide a better understanding of biofouling on different commercial membranes studied with a variety of methods. For a holistic understanding of biofouling mechanisms in real operational conditions it is important to assess all the characteristics of the membranes that affect it, such as hydrophobicity, surface charge, roughness, topography, stiffness, etc. for a wider range of membranes, including the use of additives. Also, information on the separating layer of commercial membranes is not sufficient for a full interpretation of membrane performance, as the performance also depends on the support layer and on the solvent used for the dissolution of the polymer during the synthesis of the membranes [39]. Moreover, further studies of a wider variety of fouling agents, both proteins and bacteria (including gram-positive bacteria and eventually a natural microbial consortium) with different hydrophobicity levels are strongly recommended. The use of the dynamic setup was an important step towards studying a multitude of operating conditions, because it has been reported that bacterial adhesion has not been studied thoroughly under pressure [21].

Furthermore, it is important to develop new and improve the existing non-destructive techniques for real-time *in-situ*

determination of biofouling during the continuous operation of membrane modules. Such examples are the measurement of biofilm thickness with the use of ultrasonic time-domain (UTDR) and frequency-domain (UFDR) reflectometry techniques [40], surface-enhanced real-time Raman spectroscopy (SERS), which also allows the differentiation of fouling types and their changes over time [41], or optical coherence tomography (OCT), a technique which uses back-scattered light to produce real-time dynamic cross-sectional images of the fouling layer [42]. Innovative bacterial growth potential methods have also been developed to monitor the fouling potential in reverse osmosis systems [43,44].

All these efforts are important for the design of membranes with antifouling properties with the aim to lower environmental impact and provide affordable water of good quality.

4. Conclusions

Under the studied conditions, in all static and dynamic experiments, higher levels of BSA and *E. coli* were adhered on the hydrophilic membranes (PES and nylon) compared to the hydrophobic ones (PTFE and PVDF). This observation was explained based on the hydrophilic nature of both fouling agents and leads to the conclusion that the hydrophobicity of potential fouling agents should be taken into account before assessing the antifouling properties of membranes.

In terms of methodology, although the static methods are easier and faster for studying protein fouling, the dynamic ones provide a better understanding of the mechanisms involved in real operational conditions. Furthermore, for bacterial enumeration, swabbing provides a good estimation of the actual population of bacteria adsorbed on the membranes, while incubation of membranes in LB medium can detect the presence of lower numbers of bacteria attached but it only provides a comparative analysis and not the actual population of bacteria attached.

Symbols

R_f	—	Fouling ratio, defined as the degree of flux loss caused by fouling
J_0	—	Initial flux of the BSA solution at the beginning of the batch test, L m ⁻² h ⁻¹
J_{30}	—	Flux of the BSA solution after 30 min run time, L m ⁻² h ⁻¹

Acknowledgments

This paper is supported by ERA-NET MED 2-72-357 project IDEA (Development of a solar powered, zero liquid discharge Integrated Desalination Membrane System to address the needs for water of the Mediterranean region). Dr. Scoullou and Mr. Tournis would like to acknowledge European Union's Horizon 2020 research and innovation programme under grant agreement No 958454, project intelWATT (Intelligent Water Treatment for water preservation combined with simultaneous energy production and material recovery in energy intensive industries) for partial funding of this research.

References

- [1] A.A. Sapalidis, E.P. Kouvelos, G.E. Romanos, N.K. Kanellopoulos, Introduction to membrane Desalination, A.A. Sapalidis, Ed., Membrane Desalination, CRC Press, New York, 2020. Available at: <https://doi.org/10.1201/9780429020254>
- [2] J. Yin, B. Deng, Polymer-matrix nanocomposite membranes for water treatment, *J. Membr. Sci.*, 479 (2015) 256–275.
- [3] M. Padaki, R. Surya Murali, M.S. Abdullah, N. Misdan, A. Moslehyani, M.A. Kassim, N. Hilal, A.F. Ismail, Membrane technology enhancement in oil–water separation. A review, *Desalination*, 357 (2015) 197–207.
- [4] A. Subramani, M. Badruzzaman, J. Oppenheimer, J.G. Jacangelo, Energy minimization strategies and renewable energy utilization for desalination: a review, *Water Res.*, 45 (2011) 1907–1920.
- [5] R. Zhang, Y. Liu, M. He, Y. Su, X. Zhao, M. Elimelech, Z. Jiang, Antifouling membranes for sustainable water purification: strategies and mechanisms, *Chem. Soc. Rev.*, 45 (2016) 5888–5924.
- [6] P.S. Goh, W.J. Lau, M.H.D. Othman, A.F. Ismail, Membrane fouling in desalination and its mitigation strategies, *Desalination*, 425 (2018) 130–155.
- [7] H.-C. Flemming, Microbial Biofouling: Unsolved Problems, Insufficient Approaches, and Possible Solutions, H.-C. Flemming, J. Wingender, U. Szewzyk, Eds., Biofilm Highlights, Springer Series on Biofilms, Springer, Berlin, Heidelberg, 2011, pp. 81–109. Available at: https://doi.org/10.1007/978-3-642-19940-0_5
- [8] R. Komlenic, Rethinking the causes of membrane biofouling, *Filtr. Sep.*, 47 (2010) 26–28.
- [9] S.S. Bucs, N. Farhat, J.C. Kruijthof, C. Picioreanu, M.C.M. van Loosdrecht, J.S. Vrouwenvelder, Review on strategies for biofouling mitigation in spiral wound membrane systems, *Desalination*, 434 (2018) 189–197.
- [10] C. Abrusci, D. Marquina, A. Santos, A. Del Amo, T. Corrales, F. Catalina, Biodeterioration of cinematographic cellulose triacetate by *Sphingomonas paucimobilis* using indirect impedance and chemiluminescence techniques, *Int. Biodeterior. Biodegrad.*, 63 (2009) 759–764.
- [11] K.J. Chinu, A.H. Johir, S. Vigneswaran, H.K. Shon, J. Kandasamy, Biofilter as pretreatment to membrane based desalination: evaluation in terms of fouling index, *Desalination*, 247 (2009) 77–84.
- [12] D. Kim, G.L. Amy, T. Karanfil, Disinfection by-product formation during seawater desalination: a review, *Water Res.*, 81 (2015) 343–355.
- [13] S.F. Anis, R. Hashaikh, N. Hilal, Reverse osmosis pretreatment technologies and future trends: a comprehensive review, *Desalination*, 452 (2019) 159–195.
- [14] L.D. Tijjing, Y.C. Woo, J.-S. Choi, S. Lee, S.-H. Kim, H.K. Shon, Fouling and its control in membrane distillation—a review, *J. Membr. Sci.*, 475 (2015) 215–244.
- [15] N. Alnairat, M. Abu Dalo, R. Abu-Zurayk, S. Abu Mallouh, F. Odeh, A. Al Bawab, Green synthesis of silver nanoparticles as an effective antibiofouling material for polyvinylidene fluoride (PVDF) ultrafiltration membrane, *Polymers*, 13 (2021) 3683, doi: 10.3390/polym13213683.
- [16] S. Jeong, G. Naidu, T. Leiknes, S. Vigneswaran, In: E. Drioli, L. Giorno, E. Fontananova, Eds., *Comprehensive Membrane Science and Engineering*, 2nd ed., Elsevier, Oxford, 2017, pp. 48–71. Available at: <https://doi.org/10.1016/B978-0-12-409547-2.12261-9>
- [17] R.A. Al-Juboori, T. Yusaf, Biofouling in RO system: mechanisms, monitoring and controlling, *Desalination*, 302 (2012) 1–23.
- [18] W.S. Ang, M. Elimelech, Protein (BSA) fouling of reverse osmosis membranes: implications for wastewater reclamation, *J. Membr. Sci.*, 296 (2007) 83–92.
- [19] X. Yang, D. Li, Z. Yu, Y. Meng, X. Zheng, S. Zhao, F. Meng, Biochemical characteristics and membrane fouling behaviors of soluble microbial products during the lifecycle of *Escherichia coli*, *Water Res.*, 192 (2021) 116835, doi: 10.1016/j.watres.2021.116835.
- [20] L. Yu, Y. Zhang, B. Zhang, J. Liu, H. Zhang, C. Song, Preparation and characterization of HPEI-GO/PES ultrafiltration membrane with antifouling and antibacterial properties, *J. Membr. Sci.*, 447 (2013) 452–462.
- [21] O. Habimana, A.J.C. Semião, E. Casey, The role of cell-surface interactions in bacterial initial adhesion and consequent biofilm formation on nanofiltration/reverse osmosis membranes, *J. Membr. Sci.*, 454 (2014) 82–96.
- [22] L. Eykens, K. De Sitter, C. Dotremont, W. De Schepper, L. Pinoy, B. Van Der Bruggen, Wetting resistance of commercial membrane distillation membranes in waste streams containing surfactants and oil, *Appl. Sci.*, 7 (2017) 118, doi: 10.3390/app7020118.
- [23] I.N. Floros, E.P. Kouvelos, G.I. Pilatos, E.P. Hadjigeorgiou, A.D. Gotzias, E.P. Favvas, A.A. Sapalidis, Enhancement of flux performance in PTFE membranes for direct contact membrane distillation, *Polymers*, 12 (2020) 345, doi: 10.3390/polym12020345.
- [24] M. Kamaz, A. Sengupta, A. Gutierrez, Y.-H. Chiao, R. Wickramasinghe, Surface modification of PVDF membranes for treating produced waters by direct contact membrane distillation, *Int. J. Environ. Res. Public Health*, 16 (2019) 685, doi: 10.3390/ijerph16050685.
- [25] G.S. Prihandana, I. Sanada, H. Ito, M. Noborisaka, Y. Kanno, T. Suzuki, N. Miki, Antithrombogenicity of fluorinated diamond-like carbon films coated nano porous polyethersulfone (PES) membrane, *Materials*, 6 (2013) 4309–4323, doi: 10.3390/ma6104309.
- [26] A. Rahimpour, S.S. Madaeni, S. Ghorbani, A. Shockravi, Y. Mansourpanah, The influence of sulfonated polyethersulfone (SPES) on surface nano-morphology and performance of polyethersulfone (PES) membrane, *Appl. Surf. Sci.*, 256 (2010) 1825–1831.
- [27] X. Huang, B. Shi, B. Li, L. Li, X. Zhang, S. Zhao, Surface characterization of nylon 66 by inverse gas chromatography and contact angle, *Polym. Test.*, 25 (2006) 970–974.
- [28] N. Stafie, D.F. Stamatialis, M. Wessling, Insight into the transport of hexane–solute systems through tailor-made composite membranes, *J. Membr. Sci.*, 228 (2004) 103–116.
- [29] Y.L. Jeyachandran, E. Mielczarski, B. Rai, J.A. Mielczarski, Quantitative and qualitative evaluation of adsorption/desorption of bovine serum albumin on hydrophilic and hydrophobic surfaces, *Langmuir*, 25 (2009) 11614–11620.
- [30] L. Zhang, G. Chowdhury, C. Feng, T. Matsuura, R. Narbaitz, Effect of surface-modifying macromolecules and membrane morphology on fouling of polyethersulfone ultrafiltration membranes, *J. Appl. Polym. Sci.*, 88 (2003) 3132–3138.
- [31] K.-H. Choo, C.-H. Lee, Effect of anaerobic digestion broth composition on membrane permeability, *Water Sci. Technol.*, 34 (1996) 173–179.
- [32] L. Chen, Y. Tian, C.-q. Cao, J. Zhang, Z.-n. Li, Interaction energy evaluation of soluble microbial products (SMP) on different membrane surfaces: role of the reconstructed membrane topology, *Water Res.*, 46 (2012) 2693–2704.
- [33] D. Rana, T. Matsuura, Surface modifications for antifouling membranes, *Chem. Rev.*, 110 (2010) 2448–2471.
- [34] G. Reshes, S. Vanounou, I. Fishov, M. Feingold, Cell shape dynamics in *Escherichia coli*, *Biophys. J.*, 94 (2008) 251–264.

- [36] M.C. van Loosdrecht, J. Lyklema, W. Norde, G. Schraa, A.J. Zehnder, The role of bacterial cell wall hydrophobicity in adhesion, *Appl. Environ. Microbiol.*, 53 (1987) 1893–1897.
- [37] H.C. van der Mei, R. Bos, H.J. Busscher, A reference guide to microbial cell surface hydrophobicity based on contact angles, *Colloids Surf., B*, 11 (1998) 213–221.
- [38] X. Zhang, Q. Zhang, T. Yan, Z. Jiang, X. Zhang, Y.Y. Zuo, Quantitatively predicting bacterial adhesion using surface free energy determined with a spectrophotometric method, *Environ. Sci. Technol.*, 49 (2015) 6164–6171.
- [39] K. Boussu, B. Van der Bruggen, A. Volodin, C. Van Haesendonck, J.A. Delcour, P. Van der Meeren, C. Vandecasteele, Characterization of commercial nanofiltration membranes and comparison with self-made polyethersulfone membranes, *Desalination*, 191 (2006) 245–253.
- [40] L. Lai, L.N. Sim, W.B. Krantz, T.H. Chong, Characterization of colloidal fouling in forward osmosis via ultrasonic time-(UTDR) and frequency-domain reflectometry (UFDR), *J. Membr. Sci.*, 602 (2020) 117969, doi: 10.1016/j.memsci.2020.117969.
- [41] M. Kögler, B. Zhang, L. Cui, Y. Shi, M. Yliperttula, T. Laaksonen, T. Viitala, K. Zhang, Real-time Raman based approach for identification of biofouling, *Sens. Actuators, B*, 230 (2016) 411–421.
- [42] L. Fortunato, S. Jeong, T. Leiknes, Time-resolved monitoring of biofouling development on a flat sheet membrane using optical coherence tomography, *Sci. Rep.*, 7 (2017) 15, doi: 10.1038/s41598-017-00051-9.
- [43] N. Dhakal, S.G. Salinas-Rodriguez, J. Ampah, J.C. Schippers, M.D. Kennedy, Measuring biofouling potential in SWRO plants with a flow-cytometry-based bacterial growth potential method, *Membranes*, 11 (2021) 76, doi: 10.3390/membranes11020076.
- [44] A. Abushaban, S.G. Salinas-Rodriguez, M. Kapala, D. Pastorelli, J.C. Schippers, S. Mondal, S. Goueli, M.D. Kennedy, Monitoring biofouling potential using ATP-based bacterial growth potential in SWRO pre-treatment of a full-scale plant, *Membranes*, 10 (2020) 360, doi: 10.3390/membranes10110360.